

## Manipulation of biological cells using a microelectromagnet matrix

H. Lee, A. M. Purdon, and R. M. Westervelt<sup>a)</sup>

Department of Physics and Division of Engineering and Applied Sciences, Harvard University, Cambridge, Massachusetts 02138

(Received 27 April 2004; accepted 7 June 2004)

Noninvasive manipulation of biological cells inside a microfluidic channel was demonstrated using a microelectromagnet matrix. The matrix consists of two layers of straight Au wires, aligned perpendicular to each other, that are covered by insulating layers. By adjusting the current in each independent wire, the microelectromagnet matrix can create versatile magnetic field patterns to control the motion of individual cells in fluid. Single or multiple yeast cells attached to magnetic beads were trapped, continuously moved and rotated, and a viable cell was separated from nonviable cells for cell sorting. © 2004 American Institute of Physics. [DOI: 10.1063/1.1776339]

Manipulation of biological cells using magnetic beads is a common method in biological and biomedical studies.<sup>1</sup> Magnetic beads are micron size polymer spheres containing a large number of superparamagnetic nanoparticles. By functionalizing the bead's surface with antibodies, peptides, or lectins, magnetic beads can be attached to or engulfed by cells with high selectivity, making it possible to manipulate cells with external magnetic fields.<sup>2-4</sup> Various magnetic manipulation tools, which use macroscopic external magnets or lithographically patterned electromagnets as the magnetic field source, have been developed for specific experimental purposes.<sup>5-8</sup>

Using a microelectromagnet matrix<sup>9</sup> combined with a microfluidic channel, we report in this letter versatile and noninvasive methods for manipulating biological cells. Specifically, we demonstrate the manipulation of individual yeast cells attached to a magnetic bead: a single cell was trapped and moved continuously, the motion of multiple cells was independently controlled for cell sorting, and cells were rotated in fluid. A protocol was developed to attach magnetic beads to yeast and the cells were stained to identify their viability during manipulation.

The capabilities of a microelectromagnet matrix to control individual biological cells make it possible to conduct new types of biological and biomedical studies. For example, magnetically tagged cells can be assembled to grow artificial tissues on micrometer length scales,<sup>10</sup> or cells can be sorted to desired locations according to their characteristics. Strong and localized force produced by the matrix can also pull or twist magnetic beads attached to cells to measure the mechanical properties of cell membrane,<sup>11</sup> or characterize the adhesion of cells to external surfaces.<sup>12</sup> Because the magnetic field patterns created by the matrix can be dynamically changed during experiments, sophisticated manipulation of cells can be performed inside a microfluidic channel.

Figure 1 shows a schematic and micrographs of a microelectromagnet matrix fabricated on a Si/SiO<sub>2</sub> substrate. As shown in Figs. 1(a) and 1(b), a matrix has two sets of straight conducting wires aligned perpendicular to each other. Each layer of conducting wires is covered with an insulating layer [Fig. 1(c)] to prevent electrical shorting between wires. The conducting wires were patterned either by optical lithogra-

phy or by electron-beam lithography, depending on the wire pitch  $p$  required for experiments. To trap a single cell, the wire pitch should be comparable to the size of the magnetic bead attached to the cell. To provide a flat surface for cell manipulation, bisbenzocyclobutene (BCB), a resin with good planarization properties, was used to form the insulating layers. Furthermore, the total thickness of the insulating layers was  $d \geq 0.35p$  to enable the creation of a peak in the magnetic field magnitude between two adjacent wires. To control the flow of solution containing cells, a microfluidic channel was separately fabricated with poly(dimethylsiloxane) (PDMS) using soft lithography<sup>13</sup> and sealed over the surface of the microelectromagnet matrix.

When current is applied to the wires, the microelectromagnet matrix generates a strong, local magnetic field capable of trapping and moving a magnetic bead in fluid. The

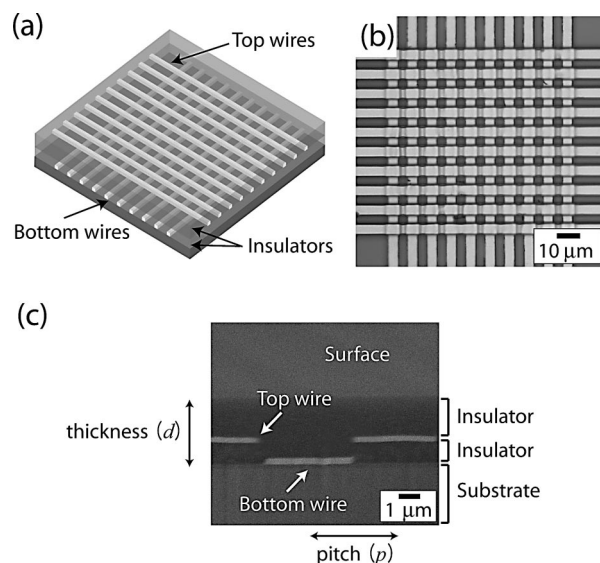


FIG. 1. (a) Schematic of the microelectromagnet matrix before attaching the microfluidic channel. Two layers of conducting wires are aligned perpendicular to each other, separated and topped by insulating layers. (b) Micrograph of a matrix with 10 Au wires in each layer of conductors (a  $10 \times 10$  matrix). The width and the pitch of the wires are 4 and 8  $\mu\text{m}$ , respectively. (c) Cross section of the matrix along a diagonal direction. The top and bottom wires are indicated along with the substrate, two insulating layers, and the top surface. The total thickness of insulating layers was  $d \geq 0.35p$  to allow the creation of a peak in the magnetic field magnitude between two adjacent wires.

<sup>a)</sup>Electronic mail westervelt@deas.harvard.edu

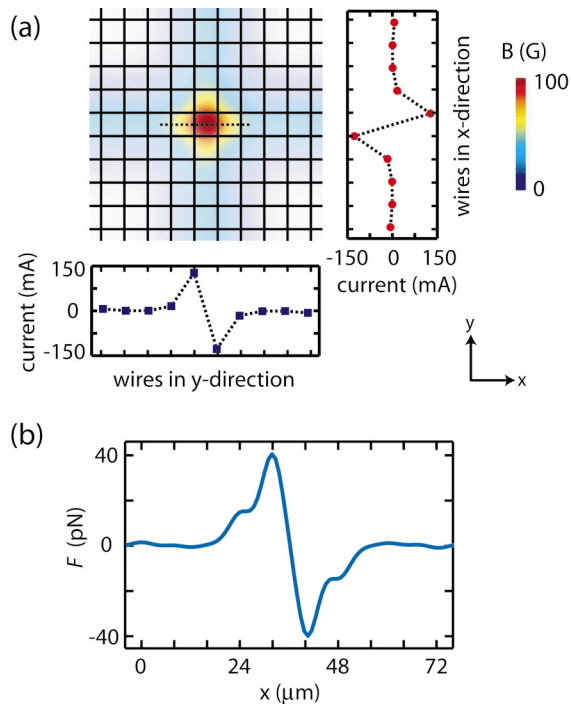


FIG. 2. (Color) Magnetic field pattern and force profile computed for a  $10 \times 10$  matrix and a magnetic bead. (a) A single peak in the magnetic field magnitude is shown with the currents value of each wire. Currents were optimized to generate a Gaussian shaped peak ( $B=10$  mT). The solid lines show wire positions and the color bar scale corresponds to the magnetic field magnitude. (b) The force on a trapped magnetic bead is shown along the dotted line in (a). A large force ( $\sim 40$  pN) on the bead allows the matrix to move cells attached to the bead on the surface of the device.

potential energy of a trapped bead and the trapping force on the bead are  $U = -\mathbf{m} \cdot \mathbf{B}$  and  $\mathbf{F} = -\nabla U = \mathbf{m} \cdot \nabla \mathbf{B}$ , respectively, where  $\mathbf{m}$  is the magnetic moment of the bead and  $\mathbf{B}$  is the magnetic field from the matrix. Due to the superparamagnetic nature of the bead, the magnetic moment is proportional to the external field,  $\mathbf{m} = V\chi\mathbf{B}/\mu_0$ , where  $V$  is the volume of the bead,  $\chi$  is the magnetic susceptibility of the bead, and  $\mu_0$  is the permeability in a vacuum. The potential energy and the trapping force of the matrix are  $U = -V\chi B^2/\mu_0$  and  $\mathbf{F} = V\chi/\mu_0 \nabla B^2$ , respectively.

Figure 2 shows profiles for the magnetic field and trapping force calculated for the matrix and magnetic bead used in the experiments. In Fig. 2(a) a single peak ( $B=10$  mT) in the magnetic field magnitude is shown along with the current distribution in the wires. The matrix has ten wires in each layer (a  $10 \times 10$  matrix) with a wire pitch of  $8 \mu\text{m}$  [Fig. 1(b)]. The current in each wire was optimized using the least square algorithm to produce a Gaussian shaped peak in the magnetic field magnitude. The magnetic bead<sup>14</sup> has the magnetic susceptibility  $\chi=0.165$  and is  $2.8 \mu\text{m}$  in diameter. When the magnetic bead is trapped at the center of the peak, the magnitude of the potential energy is  $>10^5 k_B T$  at room temperature, where  $k_B$  is the Boltzmann constant. Because the peak is localized on micrometer length scales, a large force  $F \sim 40$  pN can be exerted on the bead as shown in Fig. 2(b). Cells attached to magnetic beads, therefore, can be stably trapped and moved by the matrix at room temperature.

Cell manipulation with the microelectromagnet matrix was performed using baker's yeast (*Saccharomyces cerevisiae*) as the target sample. Figure 3(a) shows a scanning electron microscope image of a yeast cell attached to a magnetic

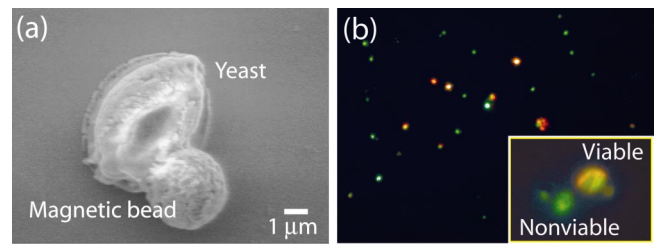


FIG. 3. (Color) (a) Scanning electron microscope image of a yeast cell (*Saccharomyces cerevisiae*) bound to a magnetic bead. The bead was coated with Concanavalin-A, which makes a specific binding to sugar molecules expressed on the wall of yeast cell. (b) Fluorescent microscope image of yeast cells stained with a two-color dye. Viable cells are exhibiting red intravacuolar structures whereas nonviable cells are diffusively green (Inset).

bead of diameter  $2.8 \mu\text{m}$ . The surface of the magnetic bead was functionalized with Concanavalin-A, a lectin that specifically binds to sugar molecules<sup>15</sup> ( $\alpha$ -D-mannose) on the yeast cell's surface with a binding force<sup>16</sup>  $\sim 100$  pN. To determine the viability of the yeast cells, a two-color fluorescent dye (FUN 1; Molecular Probes), which utilizes the metabolic differences between viable and nonviable cells for color labeling, was used for cell staining. Figure 3(b) shows a fluorescent microscope image of stained yeast cells attached to magnetic beads. Viable yeast cells were observed red with vivid cylindrical inner structures, while nonviable cells fluoresced green [Fig. 3(b) inset].

The solution containing the stained, bead-bound yeast cells was introduced into the microfluidic channel, attached to the surface of the matrix, by a low-flow peristaltic pump. Currents were supplied by 20 sources, one for each wire of the matrix, that were individually controlled by a computer. The temperature of the device was maintained at  $25^\circ\text{C}$  with active cooling by a thermoelectric cooler on the back of the devices. An epifluorescent microscope equipped with a CCD camera was used to observe the manipulation process.

Figure 4 shows a series of images that demonstrate the versatility of a matrix by manipulating single and multiple yeast cells. The optimized magnetic field patterns needed for the sophisticated control of cells in fluid were produced by adjusting the current in all 20 wires of the matrix. Figure 4(a) shows the trapping and continuous transport of a single cell with the corresponding magnetic field patterns. A single peak in the magnetic field magnitude was created and moved in steps less than the wire pitch, precisely positioning a cell with micrometer resolution. Figure 4(b) demonstrates how multiple biological cells can be controlled independently and sorted according to their characteristics. A group of yeast cells, one viable cell and two nonviable cells, were initially trapped by a single magnetic field peak. Subsequently, the single peak was split into two smaller peaks: one of the peaks held the nonviable cells, while the other peak was moved to separate the viable cell from the rest of the group, performing cell sorting on micrometer length scales. Reversing the sequences, two different cells can be assembled at one position to assay their interactions. Using time-varying currents, the matrix can twist or rotate specific target samples. As an example, Fig. 4(c) shows the rotation of two yeast cells bound to magnetic beads. Two sinusoidal currents at the same frequency  $f$  but with phase difference of  $90^\circ$  were applied to two wires crossing each other. A magnetic peak was formed at the crossing point of the wires with its

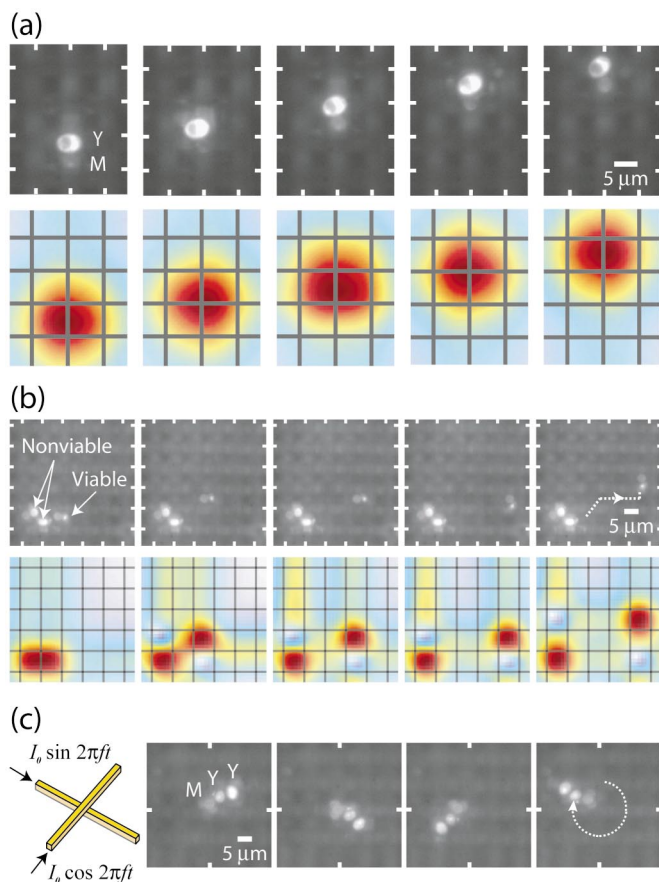


FIG. 4. (Color) Manipulation of yeast cells by the  $10 \times 10$  matrix. White ticks show wire positions. Y and M indicate yeast and magnetic bead, respectively. (a) A single peak in the magnetic field magnitude was created and moved in steps less than the wire pitch, continuously transporting a single cell. (b) Cell sorting operations with the matrix. A viable cell was separated and moved away from nonviable cells by independently controlling two magnetic peaks. (c) Two cells attached to magnetic beads were trapped and rotated by applying time-varying currents to two wires crossing each other.

direction on the surface rotating at the same frequency  $f$ . The sequence of images in Fig. 4(c) shows the rotation of two cells at  $f=2$  Hz.

The above described operations show how the microelectromagnet matrix can be a versatile tool for cell manipu-

lation. First, the matrix generates strong, localized magnetic fields, allowing stable control of individual cells in fluid. The manipulation process is noninvasive due to the biocompatibility of magnetic fields. Second, the magnetic field patterns generated by the matrix can be configured dynamically to meet a variety of experimental needs. For example, a matrix can trap, move, and position cells at desired locations where further actions can be performed; multiple cells can be moved simultaneously along different paths for cell-sorting or cell-assay. Furthermore, because the matrix is operating without external magnetic field sources or scanning instruments, it reduces the complexity and the size of an experimental setup. By integrating the matrix into microfluidic devices, chip-based experimental systems can be realized for applications in biological and biomedical studies.

The authors thank X. Zhuang and M. Bawendi for their helpful comments. This work was supported by the Nanoscale Science and Engineering Center at Harvard under NSF Grant No. PHY-0117795.

<sup>1</sup>U. Häfeli, *Scientific and Clinical Applications of Magnetic Carriers* (Plenum, New York, 1997).

<sup>2</sup>A. Radbruch, B. Mechtold, A. Thiel, S. Miltenyi, and E. Pfluger, *Methods Cell Biol.* **42**, 387 (1994).

<sup>3</sup>J. Ugelstad, P. Stenstad, L. Kilaas, W. S. Prestvik, R. Herje, A. Berge, and E. Hornes, *Blood Purif.* **11**, 349 (1993).

<sup>4</sup>A. G. Tibbe, B. G. de Groot, J. Greve, P. A. Liberti, G. J. Dolan, and L. W. Terstappen, *Nat. Biotechnol.* **17**, 1210 (1999).

<sup>5</sup>J. W. Choi, T. M. Liakopoulos, and C. H. Ahn, *Biosens. Bioelectron.* **16**, 409 (2001).

<sup>6</sup>T. Deng, G. M. Whitesides, M. Radhakrishnan, G. Zabow, and M. Prentiss, *Appl. Phys. Lett.* **78**, 1775 (2001).

<sup>7</sup>C. Haber and D. Wirtz, *Rev. Sci. Instrum.* **71**, 4561 (2000).

<sup>8</sup>C. Gosse and V. Croquette, *Biophys. J.* **82**, 3314 (2002).

<sup>9</sup>C. S. Lee, H. Lee, and R. M. Westervelt, *Appl. Phys. Lett.* **79**, 3308 (2001).

<sup>10</sup>S. N. Bhatia and C. S. Chen, *Biomed. Microdevices* **2**, 131 (1999).

<sup>11</sup>F. H. C. Crick and A. F. W. Hughes, *Exp. Cell Res.* **1**, 37 (1950).

<sup>12</sup>B. D. Matthews, D. R. Overby, F. J. Alenghat, J. Karavitis, Y. Numaguchi, P. G. Allen, and D. E. Ingber, *Biochem. Biophys. Res. Commun.* **313**, 758 (2004).

<sup>13</sup>G. M. Whitesides, E. Ostuni, S. Takayama, X. Jiang, and D. E. Ingber, *Annu. Rev. Biochem.* **3**, 335 (2001).

<sup>14</sup>Magnetic beads (Dynal M-280) used for the experiment were purchased from Dynal Biotech.

<sup>15</sup>N. Sharon and H. Lis, *Science* **177**, 949 (1972).

<sup>16</sup>A. Touhami, B. Hoffmann, A. Vasella, F. A. Denis, and Y. F. Dufrene, *Microbiology* **149**, 2873 (2003).